

# Effect of angle of approach of the forced flow on the mixed convection heat transfer in air from an infinite isothermal horizontal cylinder

M.A. Teamah and M.M. Khairat Dawood

Mechanical Eng. Dept., Faculty of Eng., Alexandria University, Alexandria, Egypt

The laminar combined convection heat transfer from an infinite isothermal horizontal circular cylinder where the forced flow can attack the cylinder at different angles from  $0^\circ$  (assisting flow) to  $180^\circ$  (opposing flow) was studied and solved numerically. The study covered a wide range of the Grashof number from 100 to  $1.69 \times 10^6$  and the Reynolds number from 40 to 300, while keeping the Prandtl number constant at  $Pr = 0.7$ . A mathematical model was constructed and solved using the Patankar-Splading Technique. A more accurate definition of the effective Reynolds number is obtained instead of the pervious definitions. The present work studies the effect of the angle of attack at different Reynolds and Grashof numbers on the Nusselt number and a correlation for the Nusselt number was obtained.

انتقال الحرارة بالحمل الرقائقي المختلط من أسطوانة أفقية لانهاية منتظمة درجة الحرارة دائرية المقطع يتواجد في الكثير من التطبيقات الهندسية. الحمل المختلط قد يتواجد فيه الحمل الجبري مؤثرا على الأسطوانة بزوايا مختلفة من صفر<sup>o</sup> (سريان مساعد للسريان الطبيعي) إلى <sup>o</sup>180 (سريان معاكس). الهدف من البحث هو دراسة مدى أكبر من قيم رينولدز و جراشوف و زوايا الإقتراب للحمل الجبري. نظرا لاستخدام الأسطوانة في الكثير من التطبيقات الهندسية التي تلزم أطوال كبيرة و بالتالي أعتبرت الأسطوانة لانهاية. حولت المعادلات التفاضلية الخاصة بالسريان و انتقال الحرارة في البعدين القطري و المماسي وأحوال الحدود إلى الصورة اللايدية. من معادلات السريان و انتقال الحرارة أستنتجت العوامل المؤثرة على انتقال الحرارة و هي : زاوية الإقتراب و أرقام جراشوف و رينولدز و براندل و بالنسبة لرقم براندل فهو ثابت للهواء و يساوي ٧,٠. تم حساب رقم نوسلت الموضعي و بتكاملة على سطح الأسطوانة نحصل على رقم نوسلت المتوسط. تم حل النموذج الرياضي حلا عدديا باستخدام طريقة عمل أتران للحجم المحدد المعروفة بباتنكر و أسبولدنغ و حدد عدد خطوات الحل التكراري المستعملة في البرنامج. جمع تأثير الحمل الجبري و الحمل الحر جمعا اتجاهيا فيما يعرف برقم رينولدز المؤثر و بالتالي تم تحويل الحمل المختلط في حالة الحمل الجبري المؤثر بزوايا إقتراب مختلفة إلى الحمل الجبري الخالص وذلك لقيم رينولدز من ٤٠ إلى ٣٠٠ و رقم رينولدز المؤثر من ٥٠ إلى ١٠٠٠. تم دراسة تأثير رقم رينولدز المؤثر و زوايا الإقتراب على رقم نوسلت المتوسط. أستنتجت العلاقة بين نوسلت المتوسط و رقم رينولدز المؤثر. رسمت أشكال تبين خطوط السريان و خطوط ثبات درجة الحرارة و كذلك قيم نوسلت الموضعي مع الزوايا المحيطة على سطح الأسطوانة وذلك لقيم رينولدز و رينولدز المؤثر و زوايا الإقتراب صفر<sup>o</sup> و ٦٠<sup>o</sup> و ١٢٠<sup>o</sup> و ١٨٠<sup>o</sup> التي تمثل الحالات المقاربة إلى الحمل الجبري و المختلط و الحر. و تبين تأثير زوايا الإقتراب و رقم رينولدز على خطوط السريان و خطوط ثبات درجة الحرارة و أيضا قيم نوسلت الموضعي مع الزوايا المحيطة. بمقارنة النتائج مع الأبحاث المنشورة سابقا و جد أن قيم نوسلت الموضعي تتغير مع زوايا الإقتراب لنفس قيم رينولدز المؤثر مما يدل على أن طريقتهما لا تعطى النتائج المتوقعة. الخلاصة نجد أنه تم تجميع الحمل الحر و الحمل الجبري بزوايا اقتراب مختلفة و الذين يمثلان الحمل المختلط بمعادلة اتجاهية و تحويله إلى الحمل الجبري الخالص. تم إيجاد علاقة رياضية بين نوسلت المتوسط ورقم رينولدز المؤثر.

**Keywords:** Combined convective heat transfer, Cross flow, Isothermal horizontal cylinder, Laminar convection

## 1. Introduction

The laminar convection from a heated cylinder is an important problem in heat transfer and fluid flow. It is used in countless number of engineering applications. The literature review includes few work on the combined convection heat transfer from horizontal cylinder, especially, when the forced flow attacks the cylinder at different angles. Experi-

mental investigation of mixed convection at low Reynolds number ( $Re < 0.4$ ) was reported by Collis and Williams [1] to evaluate the effect of free convection on the overall heat transfer rate from a hot wire. B.G. Van der Hegge Zijnen [2] carried out mixed flow experiments on cylinders and correlated the data by vectorial addition of the free and forced convective heat transfer Nusselt numbers as follows:

$$Nu = \left( Nu_{forced}^2 + Nu_{natural}^2 \right)^{0.5} . \quad (1)$$

The experiments were carried out on cross flow but the agreement between the equation and the experimental data was unsatisfactory. Joshi and Sukhatme [3] obtained theoretically the local heat transfer rate from a horizontal cylinder to a transverse flow by mixed convection, assuming a thin curved boundary-layer around the cylinder at sufficiently large Reynolds and Grashof numbers and using a method similar to the cases of mixed convection along a plane wall. A.P. Hatton et al. [4] introduced the concept of a Reynolds number in case of natural convection equals  $\sqrt{2Gr}$ , and added it vectorially to the pure forced convection Reynolds number to give an effective Reynolds number for the mixed convection as follows:

$$Re_{eff}^2 = Re^2 \left[ 1 + 3.4 \sqrt{\frac{Ra}{Re^2}} \cos \varphi + 2.85 \frac{Ra}{Re^2} \right] . (2)$$

His experimental research was initiated by the requirement to measure the low speed air velocities that occur in natural convection. The measurements of the average Nusselt numbers for electrically heated horizontal cylinders covered the ranges  $10^{-2} < Re < 40$  and  $10^{-3} < Gr < 10$ . A correlation for the mixed convection flow was suggested. Sharma and Sukhatme [5] investigated experimentally high Reynolds numbers up to  $5 \times 10^3$  and Grashof number up to  $7 \times 10^3$ . In their work, a criterion for the transition from free to combined to forced convection is suggested. P.H. Oosthuizen and S. Madan [6] measured the assisting flow mixed convection Nusselt number in the forced convection Reynolds number range 200 to 3000 and Grashof number from  $2.5 \times 10^4$  to  $3 \times 10^5$ . The experimental results were correlated for the average Nusselt number. The influence of flow direction on combined heat convection from a horizontal cylinder to air was studied experimentally by Oosthuizen and S. Madan [7]. They investigated the effect of four angles only ( $\varphi = 0, 90, 135$  and  $180^\circ$ ). But no general correlation was given. Jackson and H. Yen [8] obtained a correlation, which is a combination of

simplified forced and free convection equations, where the forced convection acts in the same direction of the free convection with the following form:

$$\frac{Nu}{Nu_{forced}} = 1 + \frac{Gr^{0.25}}{Re^2} , \quad (3)$$

$$Nu_{forced} = 0.5 Re_{forced}^{0.5} . \quad (4)$$

J.H. Merkin [9] studied the combined convection in both cases of heated and cooled cylinders. M. Badr [10, 11] solved the problem of combined convection heat transfer from an isothermal circular cylinder in the cases of cross, assisting and opposing flows. His study was based on the solution of the full vorticity transport equation together with energy equation. For the case of cross flow, Reynolds number range was  $1 < Re < 40$  and Grashof number was up to  $Gr = Re^2$ . The assisting flow Reynolds number range was  $5 < Re < 60$  and Grashof number was  $0 < Gr < 7.2 \times 10^3$ . The opposing flow Reynolds number range was  $5 < Re < 40$  and Grashof number was  $5 < Gr < 3.2 \times 10^3$ . E.M. Sparrow and L. Lee [12] looked at the problem of the flow of a vertical stream over a heated horizontal circular cylinder. They obtained a similarity solution based on using an approximate expression for the velocity variation outside the boundary layer. The local Nusselt number distribution was only obtained in the region upstream of the point of separation (from the forward stagnation point up to an angle of  $70^\circ$ ). Abu-Hijleh [13] solved the problem of laminar mixed convection for an isothermal cylinder numerically using the finite difference method. The Reynolds number value was varied between 1 and 200 and different incoming free stream angle of attack and buoyancy parameter  $Gr/Re^2$  up to 35. The change in the average Nusselt number, relative to the case of cross flow, was up to (+20%) and (-30%) for assisting and opposing flows, respectively. T.M. Abd-El samie [14] studied the assisting and the opposing flow mixed convection for an isothermal horizontal circular cylinder. The Grashof number was varied from 0.6 to  $2 \times 10^6$  and the Reynolds number was varied from 1 to 500. He used the concept of A.P. Hatton [4] for calculating the

effective Reynolds number based on the equivalent Reynolds number in the case of pure natural convection, which equals  $(2Gr)^{1/2}$ . Recently, W.M. Mustafa [15] reported a good review for combined convection cross flow heat transfer. From the previous review, the combined convection heat transfer from a horizontal circular cylinder was not examined in wide ranges of Reynolds and Grashof numbers as well as for different angles of attack. Also few researches in this field were based on many assumptions. Therefore, this work investigates the combined heat transfer from an infinite circular cylinder numerically as it is, for example without adding vectorially the forced and natural solutions. Also this investigation studies wide ranges for the angle of attack from  $0^\circ$  to  $180^\circ$  and Reynolds number from 40 to 300. The Grashof number was varied from 100 to  $1.69 \times 10^6$  which corresponds to an effective Reynolds number from 50 to 1000.

## 2. Mathematical formulation

Consider the problem of a horizontal circular cylinder with an isothermal surface where the temperature of the wall is constant and equals  $T_w$  and free stream of temperature  $T_\infty$  and velocity  $U$ . Introducing the dimensionless variables:

$$V_r = \frac{v_r}{U}, V_\phi = \frac{v_\phi}{U}, R = \frac{r}{d},$$

$$\theta = \left[ \frac{T - T_\infty}{T_w - T_\infty} \right], P' = \frac{p}{\rho U^2} . \quad (5)$$

Inserting the above dimensionless variables in the set of equations governing the transport of mass, momentum and thermal energy in the case of combined convection, the two-dimensional governing equations for combined convection in the dimensionless form will be:

$$\left( \frac{\partial V_r}{\partial R} + \frac{V_r}{R} + \frac{\partial V_\phi}{R \partial \phi} \right) = 0 . \quad (6)$$

$$\left( V_r \frac{\partial V_r}{\partial R} + V_\phi \frac{\partial V_r}{R \partial \phi} - \frac{V_\phi^2}{R} \right) = - \frac{\partial P'}{\partial R} - \frac{Gr}{Re^2} \theta \cos \phi +$$

$$\frac{1}{Re} \left( \frac{\partial^2 V_r}{\partial R^2} + \frac{1}{R} \frac{\partial V_r}{\partial R} - \frac{V_r}{R^2} + \frac{\partial^2 V_r}{R^2 \partial \phi^2} - \frac{2}{R^2} \frac{\partial V_\phi}{\partial \phi} \right) . \quad (7)$$

$$\left( V_r \frac{\partial V_\phi}{\partial R} + V_\phi \frac{\partial V_\phi}{R \partial \phi} + \frac{V_r V_\phi}{R} \right) = - \frac{\partial P'}{R \partial \phi} + \frac{Gr}{Re^2} \theta \sin \phi +$$

$$\frac{1}{Re} \left( \frac{\partial^2 V_\phi}{\partial R^2} + \frac{1}{R} \frac{\partial V_\phi}{\partial R} - \frac{V_\phi}{R^2} + \frac{\partial^2 V_\phi}{R^2 \partial \phi^2} + \frac{2}{R^2} \frac{\partial V_r}{\partial \phi} \right) . \quad (8)$$

$$\left( V_r \frac{\partial \theta}{\partial R} + V_\phi \frac{\partial \theta}{R \partial \phi} \right) = \frac{1}{Re Pr} \left[ \frac{1}{R} \frac{\partial}{\partial R} \left( R \frac{\partial \theta}{\partial R} \right) + \frac{\partial^2 \theta}{R^2 \partial \phi^2} \right] . \quad (9)$$

The calculation domain for the combined convection problem is shown in fig. 1. The inside boundary is defined by the solid surface of the infinite isothermal horizontal circular cylinder. On this surface, the no slip condition of the fluid is assumed so that the radial and circumferential fluid velocity components have to be annihilated and the temperature of the fluid equals the uniform temperature of the cylinder  $T_w$ .

At  $R = 1/2$  and for any value of  $\phi$

$$V_r = V_\phi = 0, \theta = 1 . \quad (10)$$

The calculation domain has no solid surface to confine it on the external side as the hot cylinder does on the inside boundary. Therefore, we have to lay the external boundary at a fictitious circle in the fluid far away from the cylinder. We chose to locate this circle far enough such that radial variation of the dependent variables at its location can be neglected. We assumed that at thirty tube diameters this condition is justified. If the forced flow direction is vertically upwards, in the same direction as the pure natural convection, the flow is named an assisting flow. It is an opposing combined convection flow if the forced convection flow direction is vertically downward. In the present study, we will study the forced convection flow at any angle.

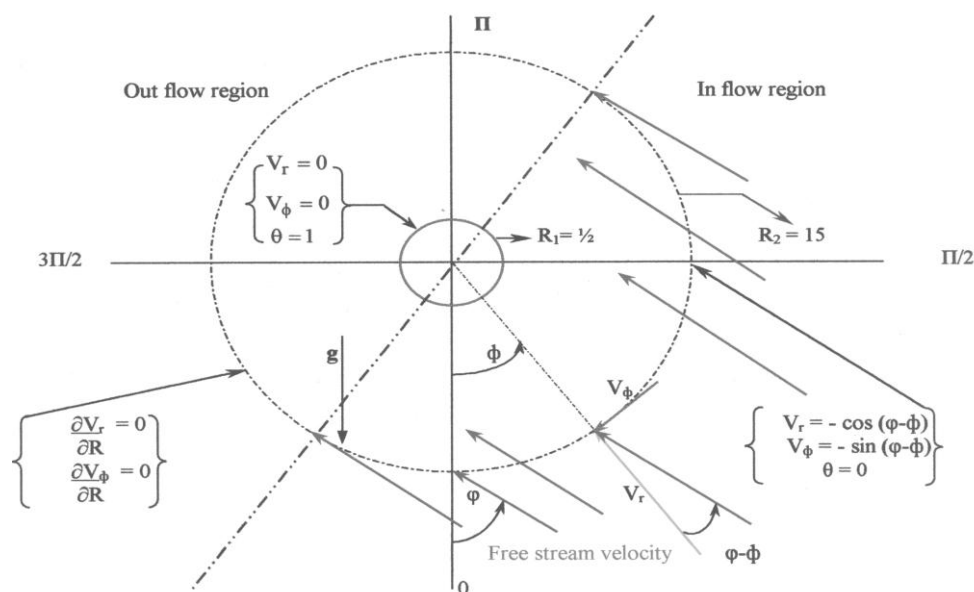


Fig. 1. Boundary condition for the combined convection flow at any angle.

Expressing the boundary conditions in terms of the dimensionless variables we obtain:

For outflow region

$$(\varphi+90 < \phi < 270+\varphi): \text{ At } R= R_2 = 15: \quad \frac{\partial V_{rv}}{\nu \partial R} = 0. \quad (11)$$

For inflow region

$$(\varphi-90 < \phi < 90+\varphi): \text{ At } R= R_2=15: \quad V_r = -\cos(\varphi-\phi), V_\phi = -\sin(\varphi-\phi), \theta=0. \quad (12)$$

The heat transfer by conduction at the outer wall of the cylinder equals the heat transfer by convection.

$$Nu_\phi = d \frac{h_\phi}{K} = - \left[ \frac{d}{T_w - T_\infty} \right] \frac{\partial T}{\partial r} \Big|_{r=\frac{d}{2}}. \quad (13)$$

Where  $Nu_\phi$  is the local Nusselt number. Introducing the dimensionless variables, defined in eq. (5), into eq. (13) we get:

$$Nu_\phi = - \frac{\partial \theta}{\partial R} \Big|_{R=\frac{1}{2}}. \quad (14)$$

The average Nusselt number around the cylinder perimeter is obtained by integrating the above local Nusselt number over the cylinder perimeter:

$$Nu = \frac{hd}{K} = \frac{1}{2\pi} \int_0^{2\pi} \left[ - \frac{\partial \theta}{\partial R} \right] \Delta\phi. \quad (15)$$

### 2.1. The numerical solution

The number of nodes and grid spacing in both the radial and circumferential directions were examined. The number of nodes used in the solution of the problem was taken as 58 nodes in the radial direction and 280 nodes in the circumferential direction. The spacing between the nodes in the circumferential direction is constant. The spacing between the nodes in the radial direction is not uniform. The spacing between the five nodes closer to the cylinder is fine and equal. The spacing between the nodes far from the cylinder is uniform with a larger value than the previous one. The computer program used for solving the combined convection for different angles of attack is based on the finite volume technique developed by S. Patankar and D.B. Spalding [16], which is based on the discretization of the governing equations using the central differencing in space. The discretization equations were solved by the Gauss-Seidel elimi-

nation method. The iteration method used in this program is a line-by-line procedure, which is a combination of the direct method and the resulting Tri Diagonal Matrix Algorithm (TDMA). The accuracy of the solution and the number of iterations were checked.

### 3. Results and discussion

#### 3.1. The effective Reynolds number

The flow around the cylinder is the resultant of two flows, the natural and forced convections. The flow due to the pure natural convection is always vertically upwards whereas the flow due to pure forced convection can approach the cylinder at any angle as shown in fig. 2.

A.P. Hatton et al. [4] suggested that the total flow could be obtained by summing the pure natural and the pure forced flows vectorially. They defined an equivalent Reynolds number in the case of pure natural convection equals  $\sqrt{2Gr}$ . Therefore, the equivalent Reynolds number " $Re_{eff}$ " due to the combined flow can be defined as follows:

$$Re_{eff} = \sqrt{Re^2 + 2Gr + 2Re\sqrt{2Gr}\cos\varphi} . \quad (16)$$

By examining the dimensionless momentum eqs. (7) and (8), the body force appears as a function in the dimensionless parameters  $Gr/Re^2$ , the Richardson number. From this fact we examined the equivalent Reynolds number for natural convection based on  $Re = \sqrt{Gr}$  instead of  $Re = \sqrt{2Gr}$ . We used the results of T. M.Abd-elsamie [14], the equations correlating the pure natural and the pure

forced convections. The natural convection correlating equation of [14] is given by:

$$Nu_n = \left[ 0.6 + 0.454 \left( \frac{Gr.Pr}{\left[ 1 + (0.559 / Pr)^{9/16} \right]^{16/9}} \right)^{0.15} \right]^2 . \quad (17)$$

Also the pure forced correlating eq. [15] is given by:

$$Nu_F = 0.864 + 0.216 Re^{0.612} \quad 5 \leq Re \leq 50 . \quad (18)$$

$$Nu_F = 0.864 + 0.287 Re^{0.53} \quad 50 \leq Re \leq 500 . \quad (19)$$

From eqs. (18) and (19) assuming a value for the Reynolds number for the forced flow, we can calculate a corresponding value of Nusselt number. The value of Nusselt number is substituted in eq. (17) to calculate a corresponding value of Grashof number. The values of the Reynolds number are the assumed values of the equivalent Reynolds number for natural convection. The results for these calculations are plotted in fig. 3. A curve fitting is made for the data obtained using least mean square method. The best fit for these results is as follows:

$$Re_{equ} = \sqrt{Gr} . \quad (20)$$

The equivalent Reynolds number in the case of the pure natural convection equals  $\sqrt{Gr}$  not  $\sqrt{2Gr}$  and the effective Reynolds number " $Re_{eff}$ " in the combined convection flow for an angle of attack  $\varphi$  is given by adding vectorially the pure forced Reynolds number and the square root of Grashof number. The summation is defined as follows:

$$Re_{eff} = \sqrt{Re^2 + Gr + 2Re\sqrt{Gr}\cos\varphi} . \quad (21)$$

We used this equation instead of eq. (16) given by A.P. Hatton [4] for calculating the Grashof number to give different values of the effective Reynolds number for assumed forced Reynolds number and angle of attack.

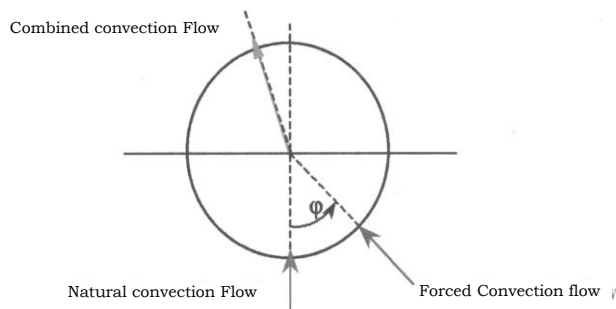


Fig. 2. Principle of the vectorial superposition of the natural and forced convection flows.

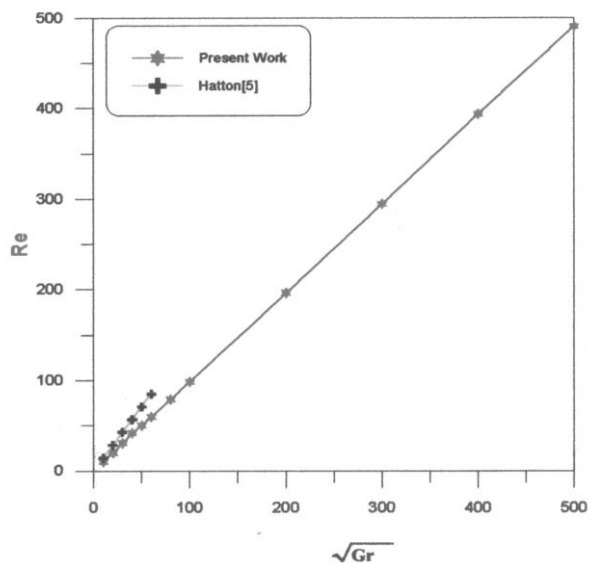


Fig. 3. The relation between the equivalent Reynolds number in case of natural convection and Grashof number.

### 3.2. Average Nusselt number

The study covers a range of the angle of attack from  $0^\circ$  to  $180^\circ$ . The fluid under consideration is air with Prandtl number,  $Pr = 0.7$ . The Reynolds number value was varied between 40 and 300 and the range of the effective Reynolds number was between 50 and 1000. For a fixed forced convection Reynolds number and effective Reynolds number, the Grashof number was calculated for selected angles of attack from eq. (21) under the condition  $Re_{eff} > Re$ . The value of the average Nusselt number is calculated from the numerically calculated results using eq. (15). The results are plotted as the average Nusselt number versus the angle of attack for different effective Reynolds numbers for Reynolds number from 40 to 300 on fig. 4. The figures show that the average Nusselt number is almost constant for a fixed effective Reynolds number and for angles of attack from  $0^\circ$  to  $180^\circ$ . The maximum deviation is 4.2 % in case of  $Re = 60$ ,  $Re_{eff} = 800$ .

These results support the appropriateness of our concept for the calculation of the effective Reynolds number, which is due to two flows, the natural convection and forced convection, so it must be constant for different angles of attack. The numerical Nusselt number data was correlated and plotted in fig. 5.

The correlation equation for the mixed convection was found to be:

$$Nu = \left( 3.46 + 2.75 \times 10^{-4} Re_{eff}^{1.448} \right). \quad (22)$$

This correlation is valid in the Reynolds number range from 40 to 300 and for the angle of forced flow attacking the cylinder from  $0$  to  $180$ . The effective Reynolds number range is from 50 to 1000 under condition  $Re_{eff} > Re$ . Fig. 5 includes the correlated average Nusselt number and the percentage difference between the correlating eq. (22) and the numerical Nusselt value. The maximum difference not exceed  $\pm 10\%$ .

### 3.3. Effect of the angle of attack on the stream, Isothermal, lines and the local Nusselt number

#### 3.3.1. In the forced convection dominated regime

The stream, isothermal lines and the local Nusselt number are shown in fig. 6, for  $Re = 40$  and  $Re_{eff} = 50$  for different angles of attack,  $0^\circ$ ,  $60^\circ$ ,  $120^\circ$ , and  $180^\circ$ . The effect of the forced convection is higher than that of the natural convection, so in this case it is considered in the forced convection dominated regime. In case (a) of  $\phi = 0^\circ$ ,  $Ri = 0.0625$  and the streamlines are directed vertically upward and the lines are not close to each other. The plume in the isothermal figure is due to the effect of the natural convection. The isothermal lines are closer to the cylinder surface, which indicates higher temperature gradient and accordingly higher heat transfer rate. The plume is directed upwards in the same direction of the forced and natural flows. The local Nusselt figure shows that the minimum value is at  $\phi = 180^\circ$  and the maximum value at  $\phi = 0^\circ$ . For angles of attack  $\phi = 60^\circ$ ,  $120^\circ$ , the stream lines are inclined according to the value of the angle of attack.

The plume in the isothermal figures is also inclined by the same value of the angle of attack. The local Nusselt figure is shifted also by the same degree of the angle of attack. In case of  $\phi = 60^\circ$  the maximum value for the local Nusselt number is at  $\phi = 60^\circ$  while the minimum value at  $\phi = 240^\circ$ . For  $\phi = 180^\circ$ , the

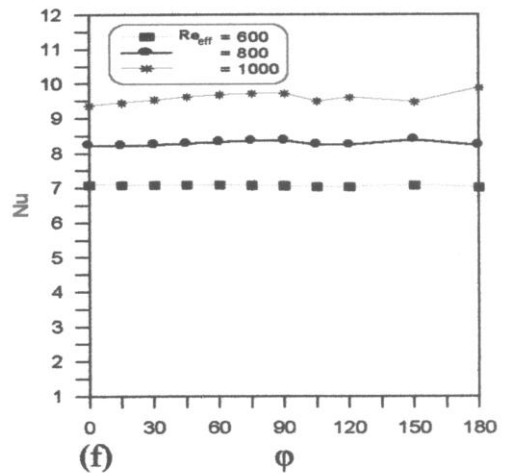
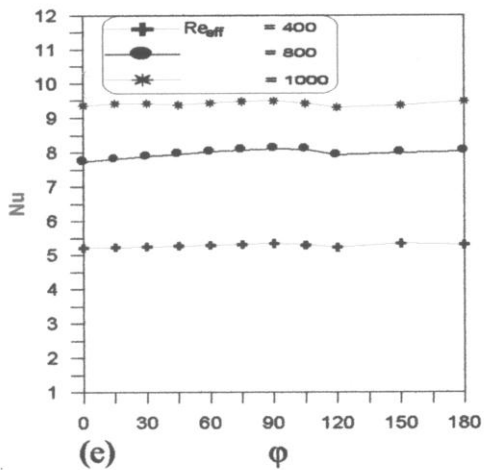
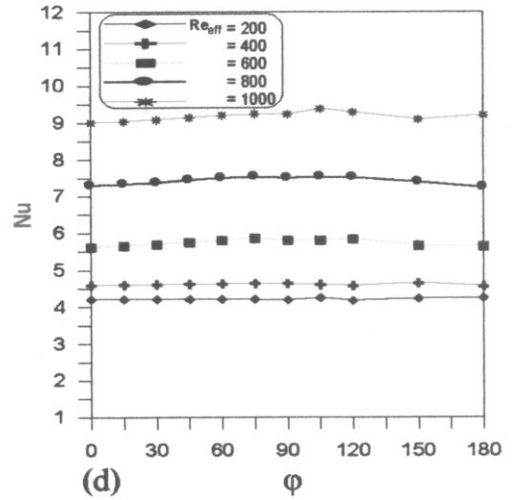
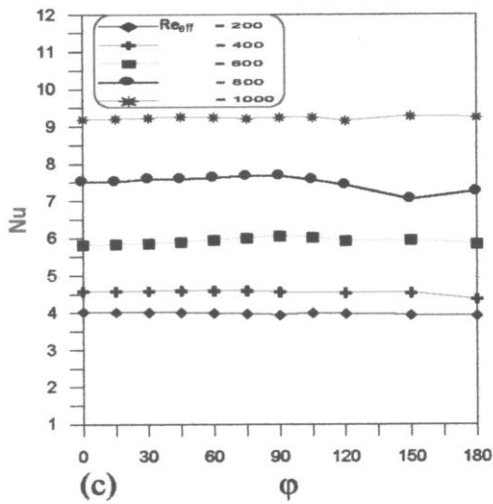
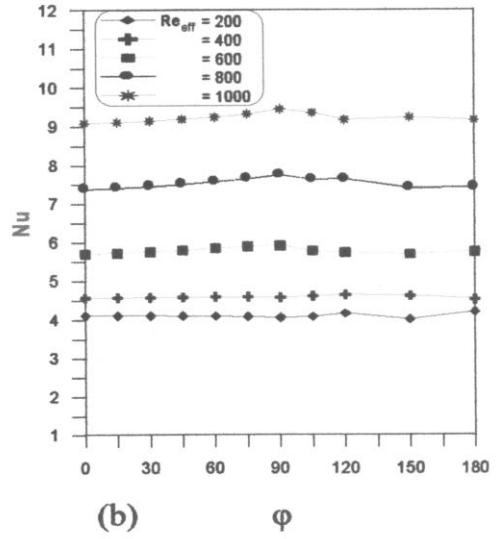
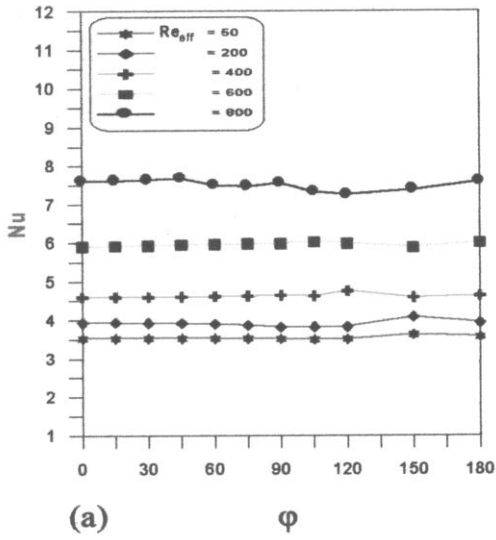


Fig. 4. The numerical average Nusselt number versus the angle of attack for mixed convection (a)  $Re = 40$ , (b)  $Re = 60$ , (c)  $Re = 80$ , (d)  $Re = 100$  (e)  $Re = 200$ , (f)  $Re = 300$ .

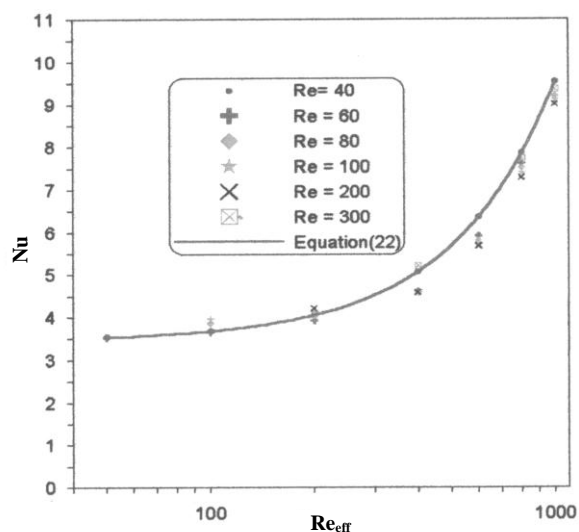


Fig. 5. The correlation of mixed convection Nusselt number.

effect of Grashof number increases slightly and the stream lines are divided into two parts as the flow is coming in the direction of the forced convection. There is a stagnation line causing the flow to pass around it. The angle of attack deflects the stream and isothermal lines according to its value. The local Nusselt figure is shifted according to the value of angle of attack and the maximum value is at the same value of the angle of attack.

### 3.3.2. In the mixed convection dominated regime

The stream and isothermal lines and the local Nusselt number are shown in fig. 7 for  $Re = 40$  and  $Re_{eff} = 200$  for different angles of attack  $0^\circ$ ,  $60^\circ$ ,  $120^\circ$ , and  $180^\circ$ . The increase of the Grashof number causes the effect of the natural convection to increase causing mixing flow with the forced convection. In figs. 7-a and 7-b for angle of attacks  $0^\circ$  and  $60^\circ$ , the stream lines are more closer to the cylinder than the case of forced convection dominated flow as a result of increasing the Grashof number causing the heat transfer rate to increase and also the local Nusselt number. The angle of attack deflects the stream and isothermal lines according to the value of the angle of attack but the effect of the natural convection is slightly felt. The local Nusselt figure shows that there are two minimum values for the local Nusselt curve as a result of the two

flows: the natural and the forced. The highest value for the local Nusselt curve is at the value of the angle of attack. The angle of attack shifts the local Nusselt curve by the same value of the angle of attack  $\phi$ . The plume and the isothermal lines in the isothermal figure are inclined according to the angle of attack as in the case of forced dominated flow but more slightly upward due to the effect of the natural convection. The stream lines also behave like the isothermal lines. In fig. 7-c for  $\phi = 120^\circ$ , the flow in the stream line figure is divided into two parts around the cylinder due to the stagnation line after the cylinder. In fig. 7-d for  $\phi = 180^\circ$ , the flow in the stream figure is divided into three parts. The first part, which is in the right hand part of the stream figure far from the cylinder in which the stream lines come in the direction of forced flow downwards with slight bend upwards due to the effect of the natural flow.

The second part is below the cylinder where there are circulating flows and stagnation lines. The circulating flow is driven by the buoyant forces and never entrained with the main flow. The third part is in the left hand part far from the cylinder which was coming with the forced flow but the stagnation line forces it to bend more than in the first part.

### 3.3.3. in the natural convection dominated regime

The stream and isothermal lines and the local Nusselt number are shown in fig. 8 for  $Re = 40$  and  $Re_{eff} = 800$  for angles of attack  $0^\circ$ ,  $60^\circ$ ,  $120^\circ$ , and  $180^\circ$ . The natural convection effect is higher than the forced convection. In the case of  $\phi = 60^\circ$ ,  $Ri = 361$  and in the case of  $\phi = 180^\circ$ ,  $Ri = 441$ . The streamlines in the case of  $\phi = 0^\circ$  are closer to each other and especially at  $\phi = 180^\circ$  due to the effect of the natural convection. The plume in the isothermal figure is not wide as in the two cases of forced dominated and mixed convections. The minimum value of the local Nusselt number is at  $\phi = 180^\circ$  and the maximum value is at  $\phi = 0^\circ$ . In the case of angle of attack of  $\phi = 60^\circ$ , the streamlines are inclined more upwards toward the vertical direction more than in the case of the mixed convection. Increasing the Grashof number causes the plume to be narrower



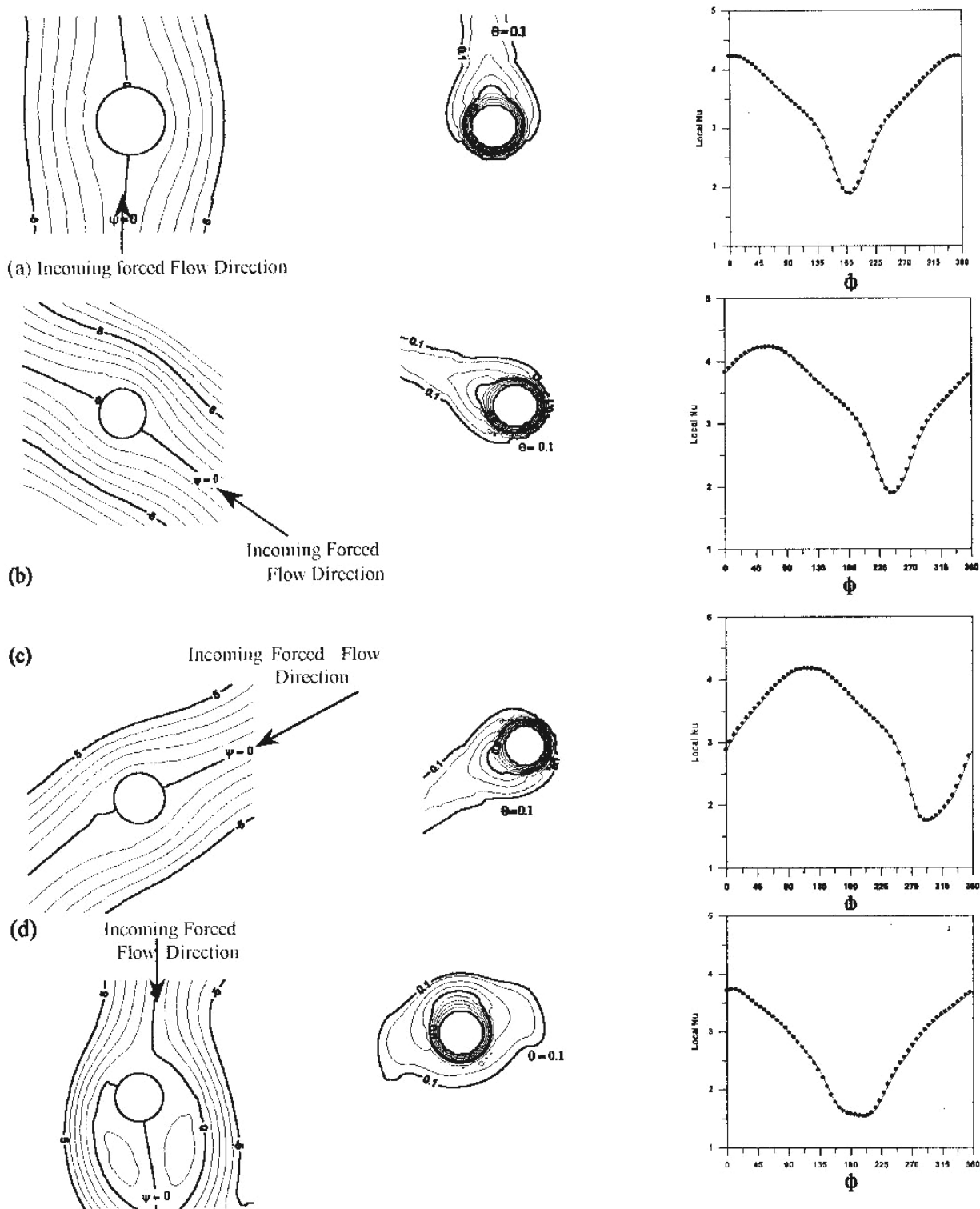


Fig. 6. Stream, isothermal lines and the local Nusselt number versus the circumferential angle (a)  $\phi = 0$  &  $Gr = 100$ , (b)  $\phi = 60$  &  $Gr = 258$ , (c)  $\phi = 120$  &  $Gr = 3.14 \times 10^3$ , and (d)  $\phi = 180$  &  $Gr = 8.1 \times 10^3$ .

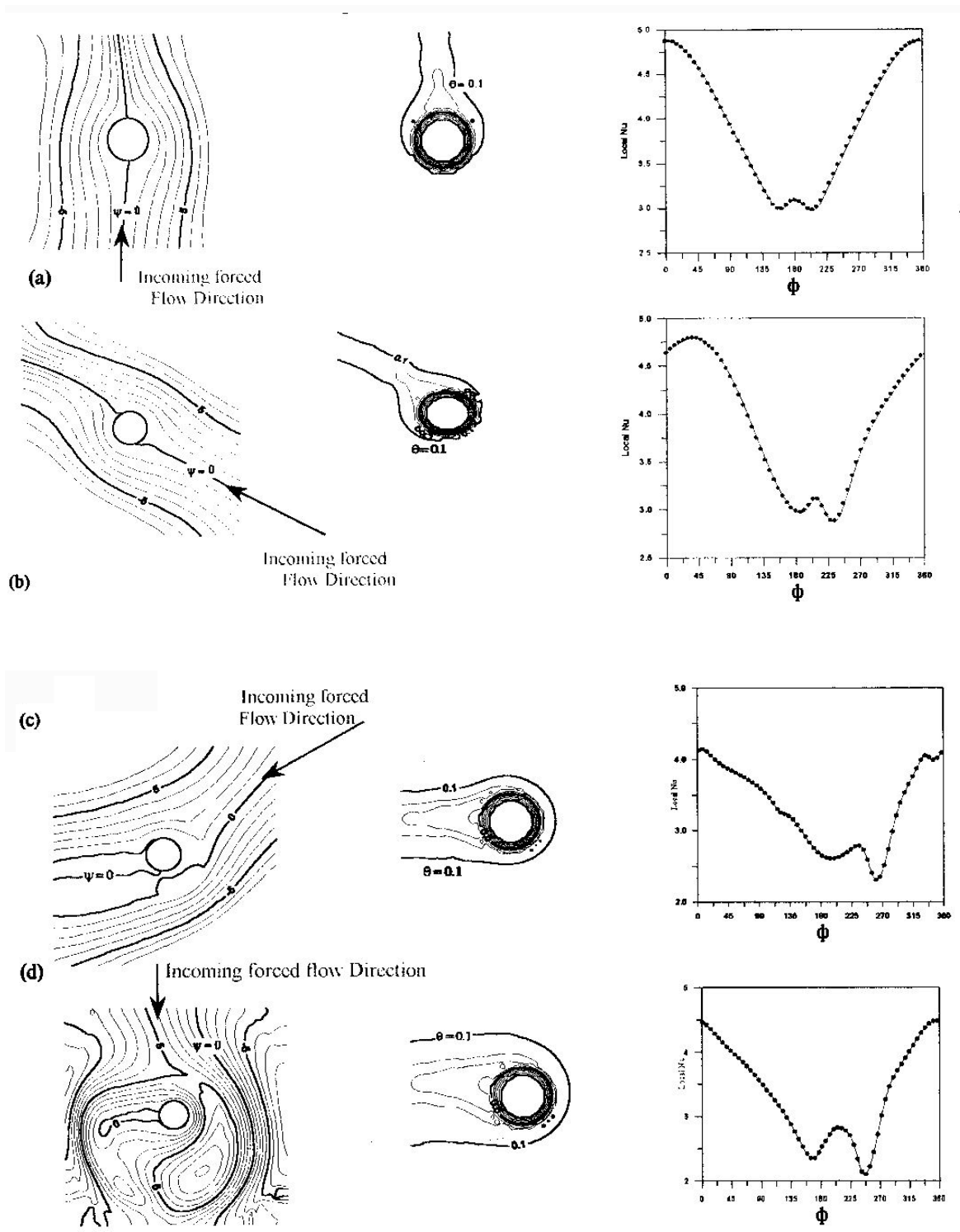


Fig. 7. Stream, isothermal lines and the local Nusselt number versus the circumferential angle (a)  $\phi = 0$  &  $Gr = 2.56 \times 10^4$ , (b)  $\phi = 60$  &  $Gr = 3.13 \times 10^4$ , (c)  $\phi = 120$  &  $Gr = 4.7 \times 10^4$ , and (d)  $\phi = 180$  &  $Gr = 5.76 \times 10^4$ .

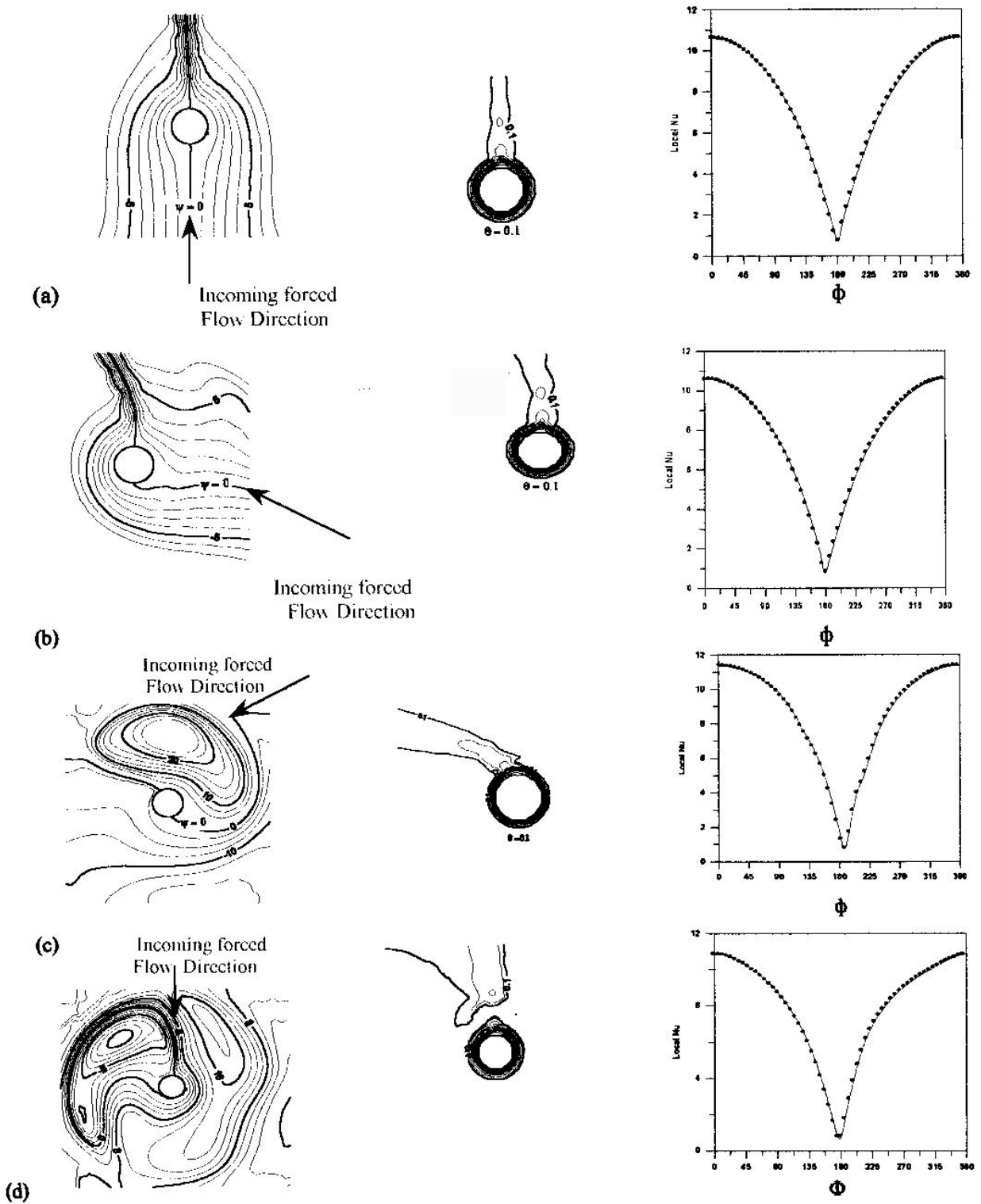


Fig. 8. Stream, isothermal lines and the local Nusselt number versus the circumferential angle (a)  $\phi = 0$  &  $Gr = 5.776 \times 10^5$ , (b)  $\phi = 60$  &  $Gr = 6.07 \times 10^5$ , (c)  $\phi = 120$  &  $Gr = 6.711 \times 10^5$ , and (d)  $\phi = 180$  &  $Gr = 7.056 \times 10^5$ .

around the cylinder and inclined to the direction of the natural convection. Increasing the angle of attack decreases the inclination of the stream and isothermal lines to the direction of the natural convection. The local Nusselt number distribution does not change due to the effect of the natural convection. In the case of  $\varphi = 120^\circ$ , the streamlines are divided into two parts. The first part, which is in the right hand part of the stream line figure and under the cylinder in which the streamlines comes as the direction of forced flow with slight inclination upwards due to the effect of the natural flow. The second part is over the cylinder where there are circulating flows and stagnation lines. In the case of  $\varphi = 180^\circ$ , the eddies get bigger than before and surround the cylinder. The local Nusselt curve does not change with the increasing of the angle of attack from  $0^\circ$  to  $180^\circ$  due to the effect of the natural convection. Increasing the angle of attack more than  $90^\circ$  causes more eddies and circulating flows in the stream line figure. The present work solved the mixed convection numerically for the whole domain from  $\Phi = 0^\circ$  to  $360^\circ$  while the pervious works solved half the domain depending on the symmetry around the line  $\Phi = 0^\circ$  as in the cases of assisting and opposing flows.

#### 4. Comparisons

Fig. 9 shows the comparison of the present work with Raithby et al. [17] who followed the

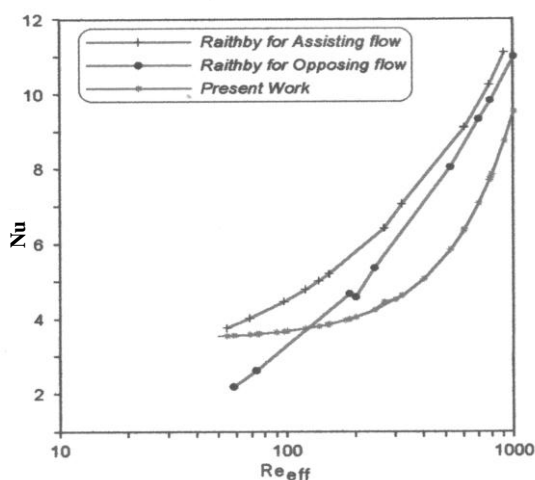


Fig. 9. Comparison of the average Nusselt number with Raithby et al. [17].

same method for calculating the effective Reynolds number as Hatton [4] using their own natural convection correlation and V.T. Morgan [18] pure forced correlation which was discussed. This method provides higher Nusselt numbers. There are significant differences between the average Nusselt number for the same effective Reynolds number in the case of assisting and opposing flow while the present work, the average Nusselt number for the same effective Reynolds number does not depend on the angle of attack.

The comparison with H.M. Badr [10,11] is plotted on fig. 10. The Nusselt numbers of H.M. Badr [10,11] are higher than those of the present work. The difference between the present Nusselt number and Nusselt number of H.M. Badr [10,11] is due to the difference between the vorticity method employed by H.M. Badr [10, 11] and the numerical technique of Patankar-Splading [16]. The present data covers a wide range of the effective Reynolds number from 50 to 1000 and Reynolds number from 40 to 300, while the work of H.M. Badr [10, 11] was for small range of the effective Reynolds number from 5 to 180 and the Reynolds number from 1 to 60.

Fig. 11 shows the comparison of the present work with A. Bassam [13] results. In his results, There is a considerable difference between the average Nusselt number for the same effective Reynolds number in the case of assisting and opposing flow  $Re_{eff} > 400$ , the difference reaches more than 20 % at  $Re_{eff} = 400$ .

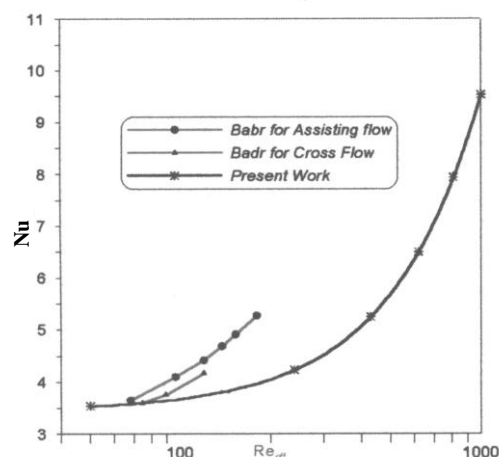


Fig. 10. Comparison of the average Nusselt with H.M. Badr [11,12].

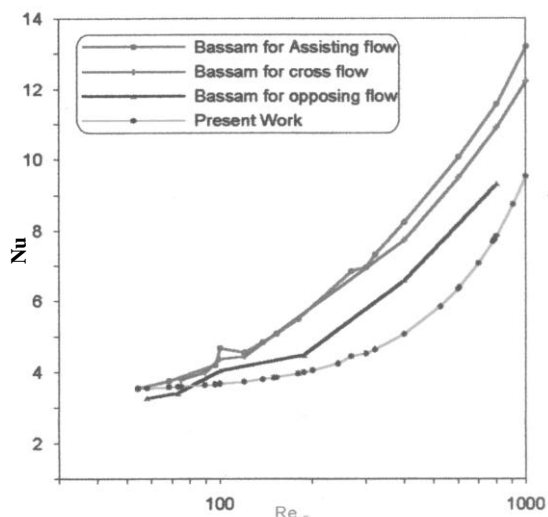


Fig. 11. Comparison of the average Nusselt with Bassam [13].

### 5. Conclusions

The combined convection heat transfer to air from horizontal circular cylinder at different angles of attack of the forced flow on the cylinder was studied. The Reynolds number was varied from 40 to 300 and the Grashof number from 100 to  $1.69 \times 10^6$  while Prandtl number was kept constant. The study covers a wide range of the angle of attack from  $0^\circ$  (which represents the assisting flow) to  $180^\circ$  (which represents the opposing flow). A more accurate definition of the effective Reynolds number was obtained by combining the natural and forced convection flows vectorially as given in eq. (21). The study shows that the equivalent Reynolds number in the case of the natural convection equals  $\sqrt{Gr}$  instead of  $\sqrt{2Gr}$  proposed previously by A.P. Hatton [5]. The study is based on the solution of the full Navier-Stokes and energy equations to construct the mathematical model. The range of the effective Reynolds number was varied from 50 to 1000 under the condition  $Re_{eff} > Re$ . The study shows that for the same Reynolds number and effective Reynolds number for different angles of attack from  $0^\circ$  to  $180^\circ$  the average Nusselt number is approximately constant which supports the proposed definition of the effective Reynolds number. The program solved the problem for the whole domain around the cylinder in the cases of the as-

sisting and opposing flows, where the previous works studied only half the domain depending on the symmetry about the vertical axis through the cylinder center. A correlation was obtained, eq. (22), that valid for Reynolds number from 40 to 300 and for effective Reynolds number from 50 to 1000. By comparing the results with previous works a insatisfactory was found and the difference was described in detail. The stream and isothermal patterns and the local Nusselt number were plotted to show some of the details of the velocity and temperature fields.

### Nomenclature

$c$	Specific heat, J/kg K,
$D$	Cylinder diameter, m,
$G$	Gravitational acceleration, m/s <sup>2</sup> ,
$Gr$	Grashof number, $g\beta (T_w - T_\infty)d^3/\nu^2$ ,
$H$	Average heat transfer coefficient, W/m <sup>2</sup> .K,
$h_\phi$	Local heat transfer coefficient at angle $\phi$ , W/m <sup>2</sup> K,
$K$	Fluid Thermal conductivity, W/m K,
$Nu$	Average Nusselt number, $h d/K$ ,
$Nu_\phi$	Local Nusselt number at angle $\phi$ , $h_\phi d/K$ ,
$P$	Pressure, N/m <sup>2</sup> ,
$P'$	Dimensionless pressure,
$Pr$	Prandtl number, $\mu c/K$ ,
$r$	Radial coordinate, m,
$R$	Dimensionless radial coordinate, $r/d$ ,
$Ra$	Rayleigh number, $g\beta (T_w - T_\infty)d^3/\nu\alpha$ .
$Re$	Pure forced convection Reynolds number, $dU/\nu$ ,
$Re_{eff}$	Effective Reynolds number,
	$Re_{eff} = \sqrt{Re^2 + Gr + 2Re\sqrt{Gr}\cos\phi}$ .
$Ri$	Richardson number, $Gr/Re^2$ ,
$T$	Local Fluid temperature, K,
$T_w$	Cylinder wall temperature, K,
$T_\infty$	Ambient temperature, K,
$\Delta T$	Temperature difference, $(T_w - T_\infty)$ , K,
$U$	Free stream forced incoming velocity, m/s,
$V_r$	Radial velocity, m/s,
$V_r$	Dimensionless radial velocity, $V_r/U$ ,
$v_\phi$	Angular velocity, m/s, and
$V_\phi$	Dimensionless angular velocity, $v_\phi/U$ .

**Greeksymbols**

$\alpha$	Thermal diffusivity, $m^2/s$ ,
$\beta$	Coefficient of volumetric thermal expansion with temperature, $K^{-1}$ ,
$P$	Local fluid density, $kg/m^3$ ,
$\rho_\infty$	Ambient fluid density, $kg/m^3$ ,
$M$	Dynamic fluid viscosity, $kg/m\ s$ ,
$Y$	Kinematic fluid viscosity, $m^2/s$ ,
$\phi$	Angular coordinate, rad,
$\theta$	Dimensionless temperature, $(T - T_\infty)/(T_w - T_\infty)$ ,
$\varphi$	Angle between the forced incoming flow direction and buoyancy force, and
$\Psi$	Stream function.

**References**

- [1] D.C. Collis and M.J. Williams, "Two-Dimensional Convection from Heated Wires at Low Reynolds Numbers," *J. Fluid*, Vol. 6, pp. 357-384 (1959).
- [2] B.G. Van der Hegge Zijnen, "Modified Correlation Formula for the Heat Transfer by Natural and by Forced Convection From Horizontal Cylinders," *Applied Scientific Research, Series A*, Vol. 6, pp. 129-140 (1956).
- [3] N.D. Joshi and S.P. Sukhatme, "An Analysis of Combined Free and Forced Convection Heat Transfer from a Horizontal Circular Cylinder to A Transverse flow," *J. Heat Transfer*, Vol. 93, pp. 441-448 (1971).
- [4] A.P. Hatton, D.D. James and H.W. Swire, "Combined Forced and Natural Convection With Low Speed Air Flow Over Horizontal Cylinder", *ASME Journal of Fluid* Vol. 42, Part 1, pp. 17-31 (1970).
- [5] G.K. Sharma and S.P. Sukhatme, "Combined Free and Forced Convection Heat Transfer from a Heated tube to a Transverse Air Stream," *J. Heat Transfer*, Vol. 91, pp. 457-459 (1969).
- [6] P.H. Oosthuizen and S. Madan, "Combined Convection Heat Transfer from Horizontal Cylinders in Air," *ASME Journal of Heat Transfer*, Vol. 92c., pp. 194-196 (1970).
- [7] P.H. Oosthuizen and S. Madan, "The Effect of Flow Direction on Combined Convective Heat Transfer from Cylinders to Air," *ASME Journal of Heat Transfer*, Vol. 14 (2), pp. 240-242 (1971).
- [8] T.W. Jackson and H.H. Yen, "Combined Forced and Free Convective Equations to Represent Combined Heat Transfer Coefficient For Horizontal Cylinders," *J. Heat Transfer*, Vol. 93, pp. 247-248 (1971).
- [9] J.H. Merkin, "Mixed Convection from a Horizontal Circular Cylinder." *Int. Journal Heat Mass Transfer*, Vol. 20, pp. 73-77 (1976).
- [10] H.M. Badr, "A Theoretical Study of Laminar Mixed Convection from a Horizontal Cylinder in a Cross Stream." *Int. Journal Heat Mass Transfer*, Vol. 26, pp. 639-653 (1983).
- [11] H.M. Badr, "Laminar Combined Convection from a Horizontal Cylinder -Parallel and Contra flow Regimes." *Int. Journal Heat Mass Transfer*, Vol. 27, pp. 15-27 (1984).
- [12] E.M. Sparrow and L. Lee, "Analysis of Mixed Convection about a Horizontal Cylinder", *Int. J. Heat Mass Transfer*, Vol. 19, pp. 232-233 (1976).
- [13] K. Abu-Hijleh, "Laminar Mixed convection Correlations for an Isothermal Cylinder in Cross flow at Different angles of Attack," *Int. Journal of Heat and Mass Transfer*, Vol. 42, pp. 1383-1388 (1999).
- [14] M. Abd-Elsamie, Heat transfer by laminar convection from an Infinite Isothermal Horizontal Circular Cylinder," M. Sc. Thesis, Mechanical Engineering, Alexandria University (1999).
- [15] W.M. Mustafa, Heat Transfer by Laminar Mixed Convection in Cross Flow From an Infinite Isothermal Horizontal Circular Cylinder to Different Prandtl Number Fluids, M. Sc. Thesis, Mechanical Engineering, Alexandria University (2001).
- [16] S.V. Patankar, *Numerical Heat Transfer and Fluid Flow*, McGraw- Hill, New York (1980).
- [17] G.D. Raithby and K.G.T. Hollands, *Handbook of Heat Transfer Fundamentals*, 2<sup>nd</sup> ed., Chap. 6, Rohsenow, Hartnett, and Ganie, eds. McGraw-Hill, New York (1985).

- [18] V.T. Morgan, the Overall Convective Heat Transfer from Smooth Circular Cylinder, *Advances in Heat Transfer*, Academic Press, Vol. 11, pp. 199-264 (1975).
- [19] M.M.K. Dawood, Effect of Angle of Approach of The Forced Flow on the Mixed Convection Heat Transfer in Air from an Infinite Isothermal Horizontal Circular Cylinder, M. Sc. Thesis, Mechanical Engineering, Alexandria University (2002).

Received September 12, 2004

Accepted November 1, 2004